

# WRAP-based nanoparticles for siRNA delivery in zebrafish embryos by simple bath immersion

Karidia Konate,<sup>1</sup> Clémentine A. Teko-Agbo,<sup>1</sup> Irène Pezzati,<sup>1</sup> Thania Hammoum,<sup>1</sup> Sébastien Deshayes,<sup>1</sup> Simon Descamps,<sup>2</sup> Eric Vivès,<sup>1</sup> Sandrine Faure,<sup>1</sup> Pascal de Santa Barbara,<sup>1</sup> and Prisca Boisguérin<sup>1</sup>

<sup>1</sup>PHYMEDEXP, University of Montpellier, INSERM U1046, CNRS UMR 9214, Montpellier, France; <sup>2</sup>Cell Biology Research of Montpellier (CRBM), University of Montpellier, UMR5237, Montpellier, France

**The use of RNA interference (RNAi) is becoming more widespread in several areas of biomedical research. However, the success of RNAi depends on the effective delivery of siRNA *in vitro* or *in vivo*. Efforts are under way to identify universally effective delivery systems. Promising candidates include cell-penetrating peptides, such as the WRAP (tryptophan and arginine-rich amphipathic peptide) family, which forms nanoparticles in the presence of short interfering RNA (siRNA). Here, we optimized the WRAP-based nanoparticles for zebrafish embryo transfection by first determining the ideal formulation compatible with the saline solution required for zebrafish embryo care. We found that adding 20% polyethylene glycol (PEG) to the WRAP1 nanoparticles provided the best nanoparticles in terms of size (around 100 nm) and uniformity ( $PdI \leq 0.3$ ), compared with other nanoparticles tested. We then performed a simple soaking procedure in which we exposed dechorionated zebrafish embryos expressing GFP in their vascular cells to siRNA-loaded 20% PEG-WRAP1 nanoparticles. Under these conditions, we showed dose-dependent siRNA internalization and efficient GFP silencing. Although still in its early stages, this proof-of-concept study provides promising prospects for further *in vivo* research in zebrafish embryos to evaluate the efficacy of gene silencing using PEGylated WRAP1 nanoparticles by skin transfection in a pathophysiological context.**

## INTRODUCTION

Besides small molecules, proteins, or antibodies, therapeutic nucleic acids (NAs) are increasingly considered as a new generation of pharmacological drugs in biomedical research.<sup>1</sup> Therapeutic NAs can be RNA or DNA molecules with different functions, specifically acting on gene regulation. Recent optimization of NA synthesis, chemical modifications, and delivery has rapidly accelerated the development of therapeutic NA. To date, 17 NA-based therapeutics have been approved by the Food and Drug Administration (FDA) or the European Medicines Agency (EMA).<sup>1</sup> In particular, double-stranded short interfering RNAs (siRNAs) have been developed as a major therapeutic tool to silence gene expression by degrading the target mRNA.<sup>2,3</sup> Today, six siRNA-based therapeutics have been approved by the FDA<sup>4</sup> with ONPATTRO (Partisiran) being the first in 2018.<sup>5</sup>

The majority of gene therapies are based on viral gene carriers, and recent years have shown both successes and challenges for this approach.<sup>6</sup> This highlights the need for a broader range of gene carriers that reduce the risk of insertional mutagenesis and potential carcinogenicity, but also allow for complex manufacturing processes and associated large-scale production. In recent decades, non-viral entities such as various naturally derived, synthetic, or hybrid (natural and synthetic) lipids, polymers, or peptides have become promising alternatives to viral carriers due to their greater genetic payload capacity, biocompatibility, and scalability.<sup>6</sup>

Cell-penetrating peptides (CPPs), usually defined as short (up to 30 amino acids) peptides, have been developed as a promising non-viral NA internalization strategy as they constitute a great alternative to the existing viral (adenovirus, retrovirus, etc.), lipid-based, or polymer-based methods.<sup>7</sup> More specifically, amphipathic or chemically modified CPPs have been increasingly used in non-covalent strategies based on electrostatic and hydrophobic interactions between both the peptide and the siRNA (Figure 1), thus opening peptides to the field of nanomedicine.<sup>8–11</sup> CPPs could be used for nanoparticle formulation in the naked version or as grafted conjugates to improve the stability and/or targeting of the nanoparticles. The most common entity used for the grafting is polyethylene glycol (PEG), which reduces the interactions between the nanoparticle and the environment.<sup>12</sup>

In this context, we designed a family of amphipathic peptides called WRAP (W- and R-rich Amphipathic Peptides), which can self-assemble into peptide-based nanoparticles (PBNs) after incubation with siRNA at a specific CPP:siRNA molar ratio (MR).<sup>13</sup> The high siRNA delivery efficacy of WRAP-PBNs in various cell lines was mainly due to their direct cellular membrane translocation, although a small fraction entered via endocytosis-dependent pathways.<sup>14</sup> Intracellular delivery of Cy3b-labeled siRNAs by WRAP-based nanoparticles was demonstrated to reach the half-maximal value (=50% of

Received 6 September 2024; accepted 27 March 2025;  
<https://doi.org/10.1016/j.omtm.2025.101458>.

**Correspondence:** Prisca Boisguérin, PHYMEDEXP, University of Montpellier, INSERM U1046, CNRS UMR 9214, Montpellier, France.

**E-mail:** [prisca.boisguerin@inserm.fr](mailto:prisca.boisguerin@inserm.fr)



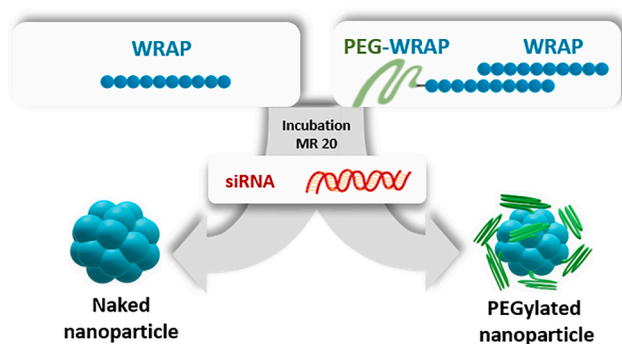


**Figure 1. Principle of the WRAP1 nanoparticle formulation as naked or PEGylated versions in the presence of siRNA**

WRAP or a mixture of PEGylated WRAP/WRAP are added to a siRNA solution at a molar ratio (MR) of 20 (e.g., 800 nM WRAP + 40 nM siRNA) to obtain nanoparticles ready for siRNA transfection.

fluorescent cells) after ~210 s of incubation and the maximal level of fluorescence (~95%) after ~15 min of incubation.<sup>13</sup> A structure-activity relationship (SAR) study revealed the major role of the N- and C-terminal leucine doublets within the WRAP peptide sequence, which are important to the nanoparticle formation in the presence of siRNA and gene silencing activity.<sup>15</sup> Based on this SAR study, two lead peptides were identified, WRAP1 (LLWRLWRL WRLWRL) and WRAP5 (LLRLLRWWRLRL), which have nearly identical delivery properties.

In the same study,<sup>15</sup> we compared the WRAP-based delivery systems with lipid-based reagents for siRNA transfection (RNAiMAX [Life Technologies], INTERFERin [PolyPlus], DharmaFect [Dharmacon], and HiPerFect [Qiagen]). Our findings demonstrated that all transfection reagents (peptide- or lipid-based) exhibited equivalent efficiency, achieving specific luciferase silencing (>80%) without any observed cytotoxic effects (lactate dehydrogenase [LDH] assay, 36 h post-transfection). However, in a long-term incubation (clonogenic assay, 14 days post-transfection), we observed some cytotoxic effects (up to 80%) for all lipid-based delivery systems, except for HiPerFect, thereby demonstrating the safety of the WRAP-based system. Finally, the first *in vivo* study performed with WRAP:siRNA nanoparticles demonstrated effective luciferase silencing in a mouse xenograft model.<sup>16</sup>

In general, the development of therapeutic molecules requires proof-of-concept studies in animal models (e.g., mice or rats). In this context, zebrafish (*Danio rerio*), initially used for decades as a classical developmental and embryological model, has received growing attention as a model for human disease and drug discovery (more than 1,700 reviews in PubMed with the keywords “zebrafish for human disease” @January 2025). The zebrafish is an excellent *in vivo* model due to (1) rapid reproduction and development, (2) high gene conservation compared with humans, and (3) a transparent body for any phenotypic visualization.

Gene regulation could be performed in zebrafish by injecting nanoparticles at different stages of development (one-cell or two-cell stage, 24 h postfertilization [hpf] or even later). However, micro-needle injections require specific materials (micro-needles, injectors, etc.) and the experimenter’s skills. Furthermore, zebrafish embryo mortality is known to be very high during the first 1–6 hpf following micro-needle injections, and the expression of specific cellular tracers (e.g., GFP, mCHERRY) required for some experiments may be too low to detect, as the expressing cell types are not developed at these early stages. Therefore, we propose a simple bath immersion protocol to perform the siRNA transfection using WRAP-based nanoparticles on dechorionated zebrafish embryos. In this context, we wanted to compare our two lead CPPs, WRAP1 and WRAP5, to determine which one is more appropriate for *in vivo* applications.

First, we evaluated the GFP silencing in HEK293 cells overexpressing GFP using different siRNA targeting different regions of the *GFP* mRNA. Afterward, we compared the size and stability of WRAP5- and WRAP1-based nanoparticles formulated in several conditions (media containing 5% glucose, 5 mM NaCl, or zebrafish culture medium) by dynamic light scattering (DLS) measurements. We selected WRAP1:siRNA nanoparticles with 20% PEGylation as the stable ones under all conditions evaluated. Finally, using a simple bathing protocol, we demonstrated the dose-dependent siRNA (Cy3-labeled) internalization and the efficient GFP silencing in dechorionated *Tg* [*flil:EGFP*]<sup>y1</sup> transgenic zebrafish embryos.

This novel application of peptide-based nanoparticles through the skin paves the way for the possible use of zebrafish embryos as an *in vivo* model for protein knockdown using vectorized siRNA in a pathophysiological context to advance the development of new therapeutic applications.

## RESULTS

### Determination of efficient siGFP-loaded WRAP nanoparticles for GFP silencing in HEK293 cells

Cells with stable expression of GFP are often used as cellular models to quantify the uptake and knockdown efficiency of developed transfection reagents. Therefore, many different siRNA sequences have been published in the literature or even proposed by various manufacturers. For this study, we selected three different siRNAs (siGFP-M,<sup>17</sup> siGFP-G,<sup>18</sup> and siGFP-W<sup>19</sup>, with the letter corresponding to the name of the first author) to evaluate their silencing properties using cellular delivery systems of the WRAP peptides we developed.<sup>13</sup> Indeed, the use of different siRNAs may lead to the induction of different silencing activities, depending on the model employed (i.e., cellular or animal). In addition, the silencing activity may be influenced by various off-target effects, which should be considered, as indicated in Figure S1. In the [supplemental information](#), details of the selection procedure for the three siRNAs (siGFP-M, siGFP-G, and siGFP-W) are highlighted.

In detail, stably GFP-transfected HEK293 cells were seeded in a microtiter plate. Twenty-four hours post-seeding, the cells were

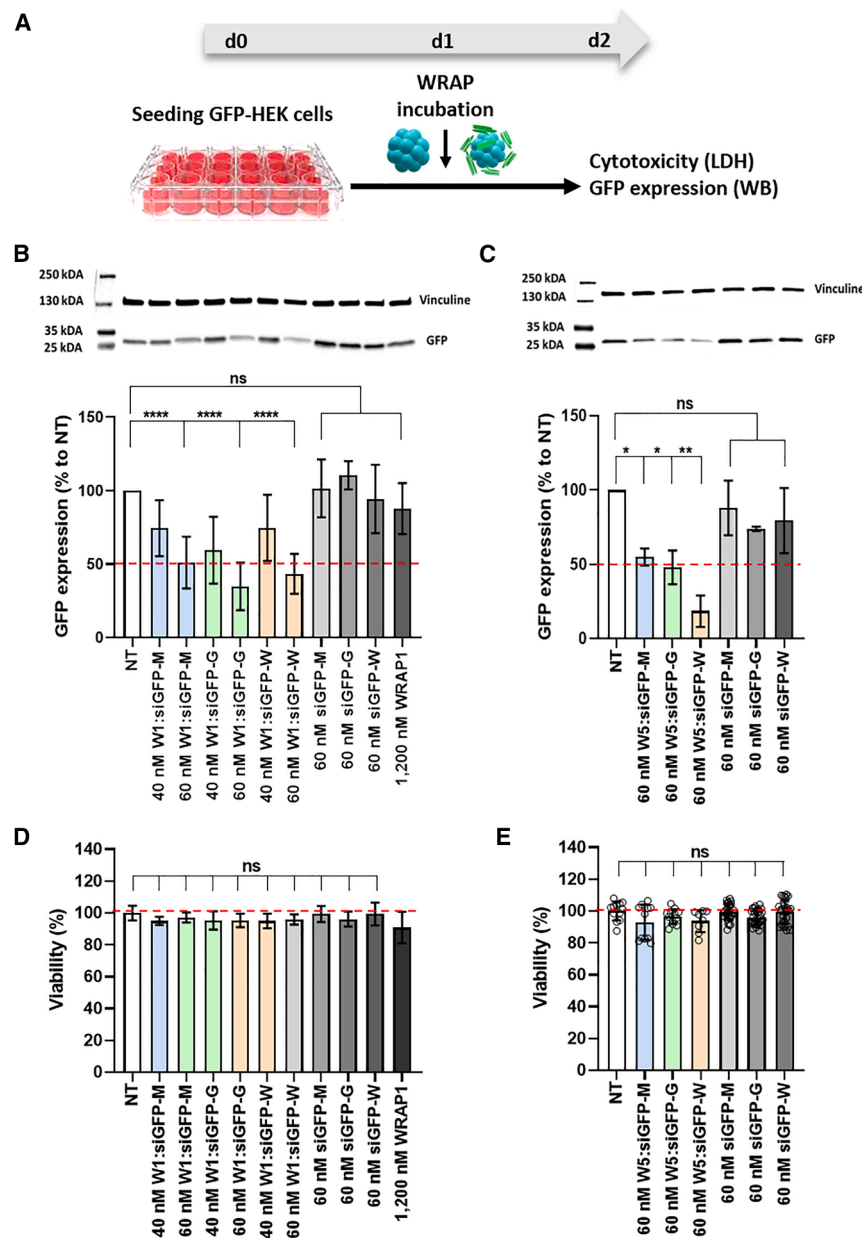


**Figure 2. Comparison of GFP silencing and cytotoxicity using different siRNA vectorized by WRAP nanoparticles**

(A) Schematic representation of WRAP:siGFP incubation protocol on GFP-overexpressing HEK293 cells. At day zero (d0), cells were seeded in a 24-well plate. Twenty-four hours post-seeding (d1), cells were incubated with the WRAP:siRNA PBNs. Twenty-four hours post-incubation (d2), supernatants were collected for cytotoxicity measurements (LDH) and afterward, cells were lysed for GFP knockdown evaluation by western blots (WB). (B and C) Western blot evaluation and quantification for WRAP1:siGFP compared with siGFP or WRAP1 alone (B) and for WRAP5:siGFP (C) compared with siGFP alone in GFP-overexpressing HEK293 cells. Data represent mean  $\pm$  SD, with  $n \geq 2$  independent experiments in duplicate. Transfection condition: Nanoparticles with MR = 20 and an siRNA concentration of 40 nM or 60 nM/Non-treated cells (NT)/Dashed line indicated 50% of GFP expression. Statistical analysis: One-way ANOVA with a Dunnett post-test, ns  $> 0.05$ , \* $p < 0.05$ , \*\* $p = 0.001$ , and \*\*\*\* $p < 0.0001$  vs. NT cells. (D and E) Viability (%) of WRAP1:siGFP compared with siGFP or WRAP1 alone (D) and for WRAP5:siGFP (E) compared with siGFP alone in GFP-overexpressing HEK293 cells. LDH release was measured from the supernatant of conditions highlighted in (B) and (C). Triton was used to determine 0% viability in the LDH assay (not shown)/Non-treated cells (NT = 100% viability)/Dashed line indicated 100% viability. Statistical analysis: One-way ANOVA with a Dunnett post-test, ns  $> 0.05$  vs. NT cells.

or the WRAP1 peptide separately, showing the importance of WRAP1-based siRNA transfection.

Subsequently, we evaluated the GFP silencing using the WRAP5 peptide as another transfection reagent. This evaluation was conducted employing the same transfection protocol and an siRNA concentration of 60 nM, which resulted in 50% silencing, as previously observed for WRAP1 (Figure 2C). Similarly, we revealed a reduction in GFP expression of around 50%

for WRAP5:siGFP-M and WRAP5:siGFP-G (\* $p < 0.05$  vs. NT cells), and even higher for WRAP5:siGFP-W (~80%, \*\* $p = 0.001$  vs. NT cells). Again, as shown for WRAP1, no GFP silencing is observed with either the siGFP or the WRAP5 peptide alone.

Finally, for all conditions analyzed by western blot, we also evaluated the potential cytotoxicity that the transfection reagent could have on the HEK293 cells by measuring the release of lactate dehydrogenase (LDH). In this context, the cytotoxicity evaluation was important to avoid false-positive results, as the toxic effect would impact the GFP expression. To normalize the assay, NT cells were used as a positive

transfected with the WRAP:siRNA complexes to evaluate the GFP silencing by western blot (Figure 2A). First, we observed knockdown efficiency for all siRNA-GFP compared with the untreated cells in our incubation condition (Figure 2B). We observed GFP silencing efficiencies of ~25% and 40% for WRAP1:siGFP-M, 40% and 65% for WRAP1:siGFP-G, and 25% and 56% for WRAP1:siGFP-W at the two siRNA concentrations used, 40 nM and 60 nM, respectively. At the highest concentration of 60 nM, the GFP knockdown was statistically significant for all used siRNA (\*\*\*\* $p < 0.0001$  vs. non-treated [NT] cells). Furthermore, no GFP silencing effect was observed when HEK293 cells were transfected with the siRNA

**Table 1. WRAP:siRNA and 20% PEG-WRAP:siRNA characterization by DLS measurements in different solutions**

Nanoparticle	Medium	Mean size (nm)	PdI
WRAP1:siRNA	5% Gluc	81.9 ± 10.5	0.387 ± 0.080
	5% Gluc +5 mM NaCl	117.2 ± 29.7	0.341 ± 0.072
	E3 medium	81.6 ± 2.1	0.323 ± 0.086
	E3 medium (d+1)	>1,000	>0.8
	5% Glucose	77.7 ± 8.6	0.255 ± 0.041
WRAP5:siRNA	5% Glucose +5 mM NaCl	>900	>0.5
	E3 medium	>500	>0.5
	E3 medium (d+1)	>1,000	>0.8
	5% Glucose	98.1 ± 19.3	0.299 ± 0.041
20PWRAP1:siRNA	5% Glucose +5 mM NaCl	128.2 ± 53.9	0.264 ± 0.049
	5% Glucose +5 mM NaCl (d+1)	122.5 ± 39.8	0.342 ± 0.088
	E3 medium	85.6 ± 9.5	0.259 ± 0.006
	E3 medium (d+1)	163.6 ± 29.1	0.327 ± 0.076
	5% Glucose	77.9 ± 4.9	0.296 ± 0.066
20PWRAP5:siRNA	5% Glucose +5 mM NaCl	128.8 ± 20.1	0.269 ± 0.057
	5% Glucose +5 mM NaCl (d+1)	ND	ND
	E3 medium	121.9 ± 71.7	0.347 ± 0.067
	E3 medium (d+1)	>1,000	>0.5
	5% Glucose	77.9 ± 4.9	0.296 ± 0.066

All WRAP:siGFP-M complexes were formed at molar ratio (MR) = 20 in an aqueous solution of 5% glucose and thereafter diluted (1:10) in the indicated medium (final peptide concentration of 10  $\mu$ M). E3 medium contains 5 mM NaCl, 0.17 mM KCl, 0.33 mM CaCl<sub>2</sub>, 0.33 mM MgSO<sub>4</sub>. Mean sizes were measured using the intensity distribution (for mean sizes by number distribution see Table S3);  $n \geq 2$  independent formulations (3 measures per run). PdI, Polydispersity Index, (d+1) = complexes were stored at 4°C and measured one day post-dilution. ND, not determined.

control (100% viability), and Triton X-100 treated cells were considered as a negative control (0% viability). Regarding the different WRAP1:siRNA conditions, all values were close to those measured for untreated cells and not lower than 95% ( $ns > 0.05$  vs. NT) (Figure 2D). The same was observed for all WRAP5:siRNA conditions ( $ns > 0.05$  vs. NT) (Figure 2E).

As previously reported, amphipathic WRAP1 and WRAP5 peptides can spontaneously form peptide-based nanoparticles (PBNs) in the presence of siRNA.<sup>13,15</sup> DLS measurements were performed to confirm similar nanoparticle sizes and polydispersity (PdI) values for all WRAP1/WRAP5 formulations performed with the three different siRNAs (Table S2; Figure S2). When formulated in an aqueous solution of 5% glucose, we observed the formation of small particles with a size of ~20–30 nm, as revealed by the size distribution based on the number (%) (Tables S2 and S3). Afterward, these small particles self-associate to the final PBN of ~80–100 nm as shown by the size distribution based on intensity (%), as previously reported.<sup>13</sup>

Considering that there are no differences among the three nanoparticles formulated with WRAP1, this suggests that their observed silencing properties in GFP-overexpression HEK293 cells are also equivalent (Figure 2B). However, at this stage, we have no explanation for the higher GFP knockdown observed for WRAP5:siGFP-W (Figure 2C) compared with the other two formulations (WRAP5:

siGFP-M and WRAP5:siGFP-G), which exhibit GFP expression reduction in the same range as shown for the three WRAP1:siGFP nanoparticles.

#### PEGylation of WRAP-based nanoparticles to provide compatibility with zebrafish medium incubation

The stability of the nanoparticles in saline solutions of different ionic forces was analyzed to evaluate the potential of WRAP-based nanoparticles as a delivery system for zebrafish embryo transfection (Table 1). For this purpose, both WRAP:siRNA nanoparticles were formulated in water and thereafter diluted (1:10) in saline solutions such as 5% glucose supplemented with 5 mM NaCl (low ionic strength) or in the zebrafish medium (E3 medium containing 5 mM NaCl, 0.17 mM KCl, 0.33 mM CaCl<sub>2</sub>, 0.33 mM MgSO<sub>4</sub>) (high ionic strength) (Table 1).

WRAP1:siRNA nanoparticles appeared to be stable after dilution in both saline solutions, i.e., we observed no change in nanoparticle size, nor aggregation or flocculation in the solution. However, the complexes were destabilized with time as reflected by the measurement 1-day post-dilution in E3 medium. In contrast, for WRAP5:siRNA, we observed the formation of large complexes or aggregates (>500 nm) with a correspondingly increased polydispersity index (PdI >0.5) in the presence of salt. The increasing PdI values correspond to a loss of particle homogeneity, which means that the variability of the detected particles can range from 100 nm small objects



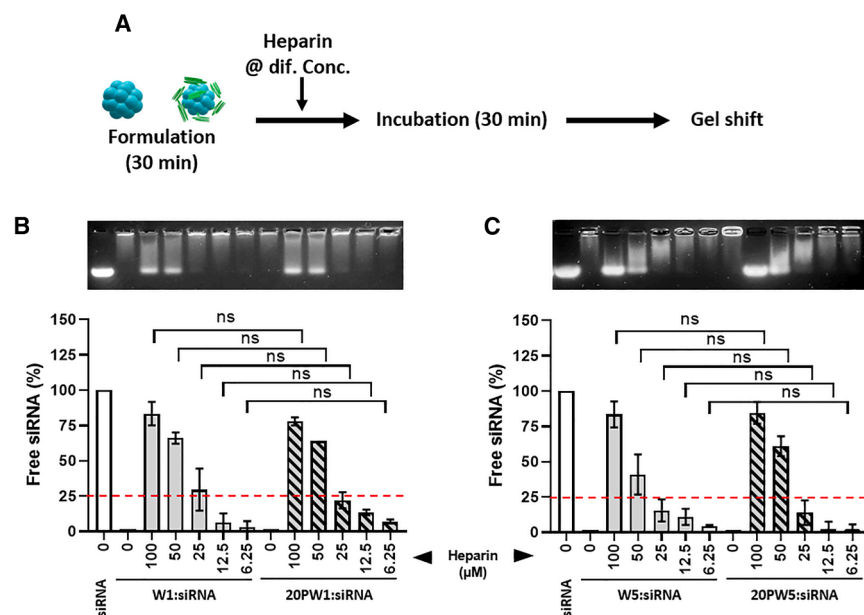


**Figure 3. Evaluation of WRAP-based nanoparticle stability in the presence of heparin**

(A) Schematic representation of incubation protocol of WRAP:siGFP-M with increasing heparin concentrations. Representative images of gel shift assays of WRAP1- (B) or WRAP5-based nanoparticles (C) incubated with heparin (100  $\mu$ M–6.25  $\mu$ M). Below the images, the graphical representations show the percentage of free siRNA normalized to siRNA alone (100%) and the nanoparticles without heparin (0%). Conditions: Nanoparticles with MR = 20 and an siGFP-M concentration of 40 nM; Dashed line indicated 25% of free siRNA; Data represent mean  $\pm$  SD, with  $n \geq 2$  independent experiments. Statistical analysis: One-way ANOVA with a Tukey multiple comparisons test,  $ns > 0.05$ .

to microparticles, making them unsuitable for cellular transfection. The differences between the two sequences are given by the number and the distribution of the tryptophan residues: WRAP1 has four tryptophan residues that are scattered all along the sequence, whereas WRAP5 has only three tryptophan residues that are clustered in the middle of the sequence. At this time, it is not clear whether the number and/or position of the tryptophan residues could impact the destabilization of the nanoparticle in the presence of ionic forces.

To confer stability to the colloidal properties of nanoparticles in the E3 medium, we sought to optimize nanoparticles by grafting protective entities. A common method to stabilize or protect the nanoparticle from interaction with serum proteins when administered via an intravenous injection<sup>20</sup> is to graft polyethylene (PEG) moieties onto nanoparticles. Based on previous results obtained with PEGylated RICK:siRNA<sup>21</sup> or PEGylated MTS-WRAP:pDNA,<sup>22</sup> we combined 20% PEG-WRAP peptide with 80% of naked WRAP peptide prior to siRNA addition and the resulting nanoparticle formation. The two nanoparticles WRAP1:siRNA or WRAP5:siRNA, formulated in an aqueous solution containing 5% glucose, have the same size as the versions containing 20% of PEG-WRAP1 or PEG-WRAP5 (Table 1). It appears that the addition of 20% PEG-peptide does not affect the nanoparticle size, as previously reported for PEG-RICK:siRNA<sup>21</sup> or for PEG-HyOMe-WRAP5:siRNA (with a pH-sensitive hydrazine linker).<sup>23</sup>

As previously done for the naked WRAP:siRNA nanoparticles, 20% PEG-WRAP:siRNA complexes were formulated in water and then diluted in both saline media (1:10 dilution) to evaluate the effect of PEGylation on nanoparticle stability. As expected, nanoparticles formulated with 20% PEG-WRAP seemed to support a higher toler-

ance to salt-containing solutions, as exemplified by both nanoparticles measured immediately after the dilution (Table 1). Twenty percent PEG-WRAP1:siRNA nanoparticles were stable in the presence of 5 mM NaCl with a size of  $128.2 \pm 53.9$  nm and a PDI of  $0.264 \pm 0.049$  as well as in E3 medium with a size of  $85.6 \pm 9.5$  nm and a PDI of  $0.259 \pm 0.006$ . Also, 20% PEG-WRAP5:siRNA nanoparticles were stable in both media with sizes of  $128.8 \pm 20.1$  nm and  $121.9 \pm 71.7$  with PDI values of  $0.269 \pm 0.057$  and  $0.347 \pm 0.067$ , respectively. However, only the WRAP1-based nanoparticles were stable even 1-day post-dilution in the E3 solution with an acceptable mean size of  $\sim 160$  nm compared with the WRAP5-based nanoparticles ( $>1,000$  nm, Table 1).

Another method of assessing the stability of nanoparticles is to evaluate them in the presence of heparin. Heparin is a linear, acidic polysaccharide belonging to the glycosaminoglycan family. It is frequently used in the field of siRNA-loaded nanoparticles to perform a competition assay with the siRNA for binding with the delivery vector (positively charged peptides or polymers). This assay also could be used to indirectly evaluate the stability of nanoparticles using gel shift assays.<sup>15,24</sup> For this purpose, nanoparticles were formulated in an aqueous solution containing 5% glucose and then supplemented with increasing concentrations of heparin (6.25  $\mu$ M–100  $\mu$ M, Figure 3A). Curiously, we observed no significant differences between naked WRAP1/5:siRNA nanoparticles and those formed with 20% PEG-WRAP1/5:siRNA with increasing heparin concentrations. Setting an arbitrary threshold of 25% free siRNA for a positive heparin impact (= siRNA release), we could show that naked or PEGylated WRAP1:siRNA nanoparticles tolerated heparin concentrations of up to 12.5  $\mu$ M (Figure 3B), whereas naked or PEGylated WRAP5-based nanoparticles tolerated higher heparin concentrations (50  $\mu$ M) (Figure 3C). The same experiments were repeated with 100% PEG-WRAP1/5 nanoparticles incubated with the same increasing heparin concentrations to confirm the nanoparticle stabilizing property of the PEG moiety (Figure S3). Indeed, fully

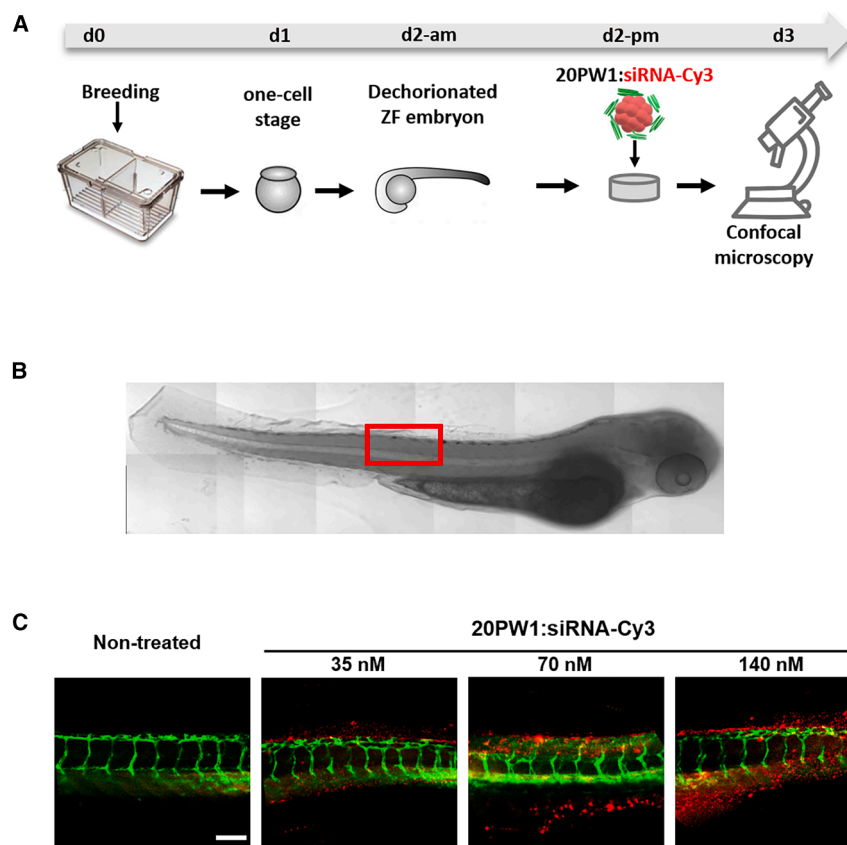


**Figure 4. Evaluation of the internalization potential of 20% PEG-WRAP1:siRNA nanoparticles in the zebrafish embryo**

(A) Schematic representation of the zebrafish embryo incubation protocol. At day zero (d0), zebrafish breeding was performed to collect one-cell stage embryos at d1. In the morning of d2 (~24 hpf), the zebrafish embryos were dechorionated and left for 6 h in E3 medium before adding in the afternoon the fluorescence-labeled 20% PEG-WRAP1:siRNA (20PW1:siRNA-Cy3) nanoparticles. After ~20 h, the embryos were washed, fixed (PFA), and imaged by confocal microscopy. (B) Visualization of the area that was used for confocal image acquisition (red square). (C) Representative images of the z stack confocal microscopy acquisition of non-treated zebrafish embryo compared with the one incubated with 20% PEG-WRAP1:siRNA-Cy3 nanoparticles at the indicated final siRNA concentrations (MR = 20). Green = GFP-expressing vascular endothelial cells, red = siRNA-Cy3. White bar = 100  $\mu$ m.

PEGylated WRAP1/5 nanoparticles released less siRNA at the same heparin concentration compared with the naked or 20% PEGylated version.

Next, the stability of the nanoparticles (WRAP1/5, 20% PEG-WRAP1/5, and 100% PEG-WRAP1/5) was evaluated by gel shift assay in saline E3 medium (data not shown). Here, we observed no siRNA release for all conditions, meaning that in the presence of salt, the nanoparticles tend to aggregate (as observed by DLS through larger sizes) without destabilizing the nanoparticle itself (aggregates are not able to migrate through the gel).

In conclusion, based on the results obtained from DLS measurements and gel shift assays, we selected the 20% PEG-WRAP1:siRNA formulation to evaluate the activity of the siRNA in a GFP-expressing zebrafish model.

#### A simple bathing incubation of zebrafish embryos with PEGylated WRAP1 nanoparticles for siRNA internalization

Gene silencing in zebrafish embryos is commonly performed by injecting oligonucleotides such as a phosphorodiamidate morpholino oligomer (PMO) at the one-cell stage. However, there is a high mortality rate at this stage (depending on the zebrafish line used) because zebrafish embryos are generally very fragile during the first 24 hpf. To avoid this delicate injection procedure, we

decided to simply bathe the dechorionated zebrafish embryos for 24 h with the PEGylated WRAP1 nanoparticles for the siRNA transfection.

For this purpose, we used zebrafish embryos derived from the breeding of a *Tg[flil:EGFP]<sup>y1</sup>* transgenic line having GFP-labeled vascular endothelial cells. Two days post-breeding, the embryos were dechorionated in the early morning, washed, and left in an E3 medium (6 h) before the addition of nanoparticles with different concentrations of Cy3-labeled siRNA. To improve GFP signal detection by confocal microscopy, embryos were treated with 1-phenyl 2-thiourea (PTU) to remove zebrafish pigmentation as reported previously.<sup>25</sup> After 20 h, zebrafish embryos were washed and fixed with PFA for confocal microscopy imaging to evaluate the potential internalization of the fluorescence-labeled siRNA (Figure 4A). Approximately the same dorsal region of the zebrafish embryo was used for z stack image acquisition by confocal microscopy (see red square in Figure 4B). For an accurate comparison of the different conditions, all images were acquired and processed using the same parameters each time.

Zebrafish embryos incubated only in an E3 medium alone showed almost no red auto-fluorescence (Figure 4C, first panel). By adding 20%-PEG-WRAP1 nanoparticles encapsulating different amounts of Cy3-labeled siRNA (35 nM, 70 nM, or 140 nM), we observed a dose-dependent accumulation of red fluorescence at the surface and within the inner regions of the zebrafish embryos (Figure 4C). To the best of our knowledge, these very encouraging results confirm for the first time, that a simple bathing procedure with the PEGylated WRAP1 nanoparticles allows the transfection of siRNA in a zebrafish embryo as a potent gene silencing strategy.

Moreover, by incubating a dechorionated zebrafish embryo with the 20% PEG-WRAP1 nanoparticles for 72 h, we confirmed that the incubation condition had no impact on zebrafish development (Figure S4). No morphological changes or differences in the embryo size were observed between untreated zebrafish embryos ( $704 \pm 12 \mu\text{m}$ ,  $n = 18$ ) and those incubated with the nanoparticles ( $702 \pm 24 \mu\text{m}$ ,  $n = 20$ ). More importantly, no zebrafish embryo died during the incubation (siRNA = 140 nM). The result showed that the nanoparticle incubation has no cytotoxic impact on the zebrafish embryos even if the nanoparticles are internalized.

#### Quantification of GFP silencing in zebrafish embryos after nanoparticle bathing

Having confirmed that siRNA internalization using 20% PEG-WRAP1 nanoparticles was possible by simply bathing the zebrafish embryos, we wanted to know if a specific GFP knockdown could be observed. In a protocol similar to that used for the siRNA-Cy3 internalization/visualization, dechorionated zebrafish embryos were incubated with 20% PEG-WRAP1:siGFP nanoparticles. Using siGFP-G as an example, the same three siRNA doses (35 nM, 70 nM, and 140 nM) were used to quantify by western blot GFP silencing after 24 h of incubation (Figure S5). However, the overwhelming presence of vitellogenin yolk proteins could potentially interfere with the identification of cellular proteins by SDS-PAGE to an unknown extent. Therefore, we performed a de-yolking procedure before the lysis of zebrafish embryos to reduce the yolk proteins in the lysate, as has been performed in several studies on zebrafish embryos and larvae at different stages postfertilization.<sup>26,27</sup>

Under these conditions, we observed a significant dose-dependent GFP silencing:  $\sim 40\%$  for 35 nM ( $**p = 0.0014$ ),  $\sim 50\%$  for 70 nM ( $****p > 0.0001$ ), and  $\sim 80\%$  for 140 nM siGFP-G ( $****p > 0.0001$ ), vs. NT, respectively (Figure S5B). In addition, we repeated the experiment and extended the nanoparticle incubation to 48 h to ensure that the correct bathing procedure was used for optimal GFP knockdown. As shown in Figure S5C, the overall GFP/ $\alpha$ -Actinin levels of the untreated and control conditions were less pronounced after 48 h of incubation compared with 24 h, probably due to the growth of the embryos (changes in the GFP/ $\alpha$ -Actinin ratios). Also, the dose-dependent GFP silencing seems to be lower:  $\sim 10\%$  for 35 nM ( $ns = 0.9630$ ),  $\sim 30\%$  for 70 nM ( $ns = 0.1451$ ), and  $\sim 50\%$  for 140 nM siGFP-G ( $*p > 0.0125$ ), respectively, vs. NT, respectively (Figure S5C).

Since the siGFP concentration of 140 nM induced the highest GFP silencing for both incubation periods, the specificity of GFP knockdown with 20% PEG-WRAP1 nanoparticles loaded with the three siGFP (siGFP-M, -G, and -W) was evaluated by western blot analyses (Figure 5A). Western blot analyses of the GFP protein expression showed a clear and specific silencing effect induced by the three PEGylated nanoparticles in the zebrafish embryos. In detail, we observed a 68% reduction in GFP expression ( $***p < 0.001$  vs. NT) for 20% PEG-WRAP1:siGFP-M, of 80% reduction ( $****p < 0.0001$

vs. NT) for 20% PEG-WRAP1:siGFP-G, and of 63% reduction ( $**p < 0.01$  vs. NT) for 20% PEG-WRAP1:siGFP-W (Figure 5B). In contrast, the applied control conditions (the three siRNAs alone or 20% PEG-WRAP1:siCtrl) had no GFP silencing properties ( $ns > 0.5$  vs. NT) demonstrating the specificity of the siRNA-loaded PEGylated nanoparticles.

#### Visualization of GFP silencing in zebrafish embryos after nanoparticle bathing

Having confirmed that a siRNA transfection using 20% PEG-WRAP1 nanoparticles was possible by simply bathing the zebrafish embryos, we wanted to know if a specific GFP knockdown could be observed. Using a protocol similar to that used for the siRNA-Cy3 internalization/visualization, dechorionated zebrafish embryos were incubated with 20% PEG-WRAP1 encapsulating the three siGFP previously tested on HEK293 cells (Figure 6A). All z stack images of the zebrafish embryos were acquired by confocal microscopy in the same dorsal region as previously described (see Figure 4B) and images were processed consistently, using the same parameters each time.

Confocal images acquired after tissue fixation showed a well-defined pattern of blood vessels due to GFP-expressing endothelial cells in untreated zebrafish embryos (Figure 5C). In contrast, the 20% PEG-WRAP1 nanoparticles encapsulating the three GFP-targeting siRNA (siGFP-M, siGFP-G, and siGFP-W) showed a remarkable reduction in green fluorescence. More importantly, this silencing appeared to be sequence-specific, as embryos incubated with the nanoparticles encapsulating a control siRNA (20% PEG-WRAP1:siCtrl) showed no reduction in the GFP signal. The importance of the drug delivery system was highlighted in embryos treated with the three GFP-targeting siRNA alone as another negative control condition showing no GFP silencing.

To obtain a more global view of the results, the green fluorescence signal intensity of each acquired image was quantified by ImageJ software. As shown in the graph (Figure 5D), we were able to quantify approximately 50% GFP silencing for the three 20% PEG-WRAP1:siGFP nanoparticles ( $**p < 0.01$  for 20% PEG-WRAP1:siGFP-G, and  $***p < 0.001$  for 20% PEG-WRAP1:siGFP-M/W vs. non-treated embryos), which was not observed with the four control conditions (3x siRNA alone or 20% PEG-WRAP1:siCtrl).

#### DISCUSSION

In this study, we established a protocol for efficient and specific gene silencing by immersing zebrafish embryos in an E3 medium containing PEGylated WRAP1-based nanoparticles encapsulating siRNA. First, we confirmed the silencing efficiency of three different published siRNAs targeting the GFP protein<sup>17–19</sup> in GFP-overexpressing HEK293 cells. Transfections were performed with the WRAP-based nanoparticles as previously described,<sup>13–15</sup> and the GFP silencing of three different siGFP-loaded nanoparticles in GFP-overexpressing HEK293 cells was evaluated by western blot in comparison to the siRNA transfection without delivery system (Figure 2). We obtained a GFP silencing of  $\sim 50\%$  for all WRAP:siGFP transfected HEK293

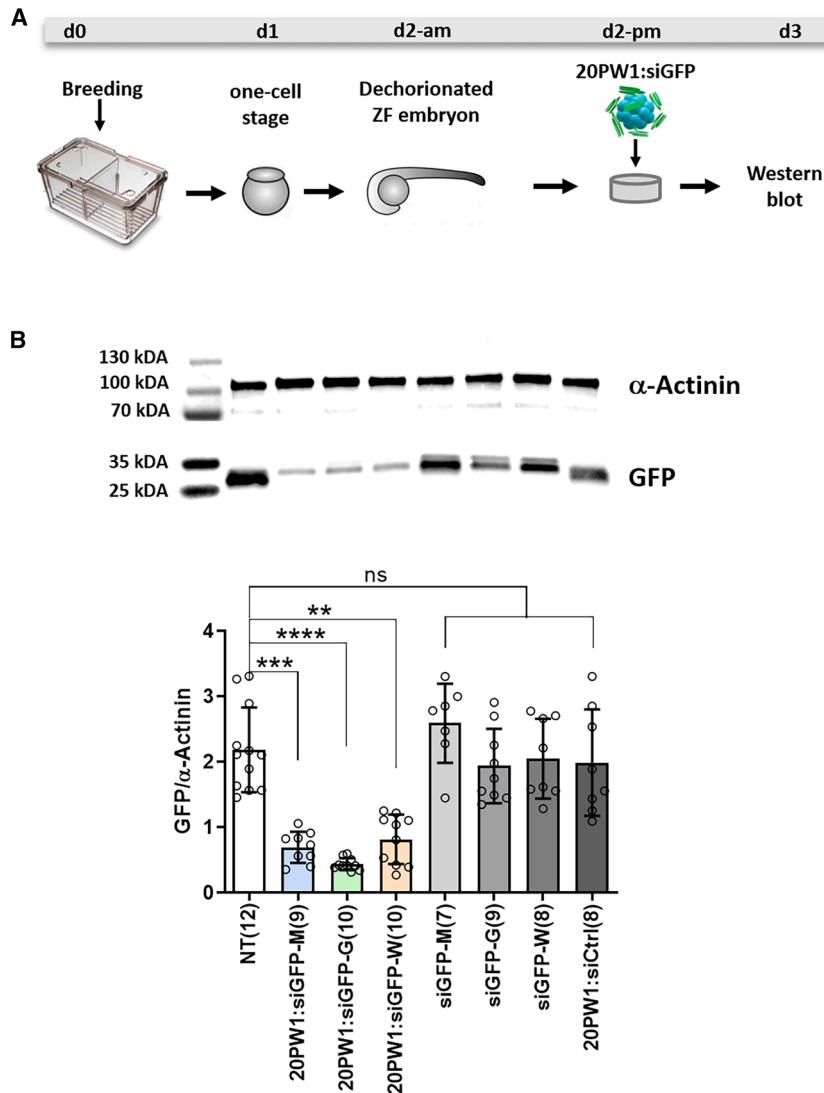


**Figure 5. Quantification of the GFP silencing in zebrafish embryos by 20% PEG-WRAP1:siRNA nanoparticle bathing**

(A) Schematic representation of the zebrafish embryo incubation protocol. At day zero (d0), zebrafish breeding was performed to collect one-cell stage embryos at d1. In the morning of d2 (~24 hpf), zebrafish embryos were dechorionated and left for 6 h in E3 medium before adding the fluorescence-labeled 20% PEG-WRAP1:siRNA (20PW1:siGFP) nanoparticles. After ~20 h, the embryos were washed, de-yolked, and lysed. Finally, proteins were quantified by western blot. (B) Representative images of western blots comparing non-treated zebrafish embryos with those incubated with 20% PEG-WRAP1:siGFP and 20% PEG-WRAP1:siCtrl nanoparticles or with the siRNA alone. The final siRNA concentration was 140 nM for all conditions (MR = 20). α-Actinin was used as a loading control. The graphical representation shows the GFP signal intensities normalized to the α-Actinin signal intensities. Brackets indicate the number of zebrafish embryos analyzed. Statistical evaluation: ns > 0.5, \*\*p < 0.01, \*\*\*p < 0.001, and \*\*\*\*p < 0.0001 vs. NT.

cells. This was consistent with the fact that wild-type GFP protein has a half-life of around 26 h,<sup>28</sup> meaning that during a 24-h incubation period for GFP knockdown, only newly synthesized GFP proteins are inhibited.

We then performed a proof of concept of *in vivo* WRAP-based siRNA transfection in *Tg[fli1:EGFP]<sup>y1</sup>* zebrafish embryos using a simple immersion method. *Tg[fli1:EGFP]<sup>y1</sup>* fish express enhanced GFP throughout the vasculature under the control of the *fli1* promoter.<sup>29</sup> To ensure the stability of the WRAP nanoparticles in the saline solution in which the zebrafish embryos were maintained, we evaluated the PEGylation of the WRAP nanoparticles. As previously reported by our team and others,<sup>21,22,30,31</sup> peptide-based nanoparticles could be improved by introducing PEG moieties on their surface to obtain a higher stabilization and/or lower interaction with molecules of the media or *in vivo* (e.g., blood or cytosol). In our case, we showed that

the addition of PEG entities (20%) increased the stability of the colloidal properties (size and Pdl) of WRAP1:siRNA nanoparticles in the presence of different saline solutions in contrast to the WRAP5:siRNA nanoparticles (Table 1). This result was further confirmed by a higher resistance to heparin of the 20% PEG-WRAP1:siRNA nanoparticles (Figure 3). Moreover, these results also emphasized the versatility of formulating such nanoparticles, which could be adapted to the ionic strength of the incubation conditions and transfection protocol.

Indeed, the ionic strength, which influences the intermolecular forces of the nanoparticles, affects the colloidal stability of the nanoparticles, leading to flocculation or precipitation phenomena based on changes in the van der Waals forces.<sup>32</sup> The negative effect of environmental salt on colloidal systems has been demonstrated for several nanoparticles, such as latex particles,<sup>33</sup> ethyl cellulose nanoparticles,<sup>34</sup> and gold nanoparticles.<sup>35</sup> Likewise, many examples have been published showing the positive effect of PEG coating on the colloidal stability of different nanoparticles such as iron oxide, gold, and SiO<sub>2</sub> but also on polymers or liposomes (see reviews in Lee<sup>36</sup>, Li et al.,<sup>37</sup> Hristov et al.,<sup>38</sup> and Shi et al.<sup>39</sup>).

Subsequently, dechorionated zebrafish embryos (24 hpf) were incubated (bathed) in an E3 medium containing the siRNA-loaded PEGylated WRAP1 nanoparticles to evaluate the feasibility of a skin transfection. First, we showed a dose-dependent internalization of the Cy3-labeled siRNA by confocal microscopy (Figure 4). Then,



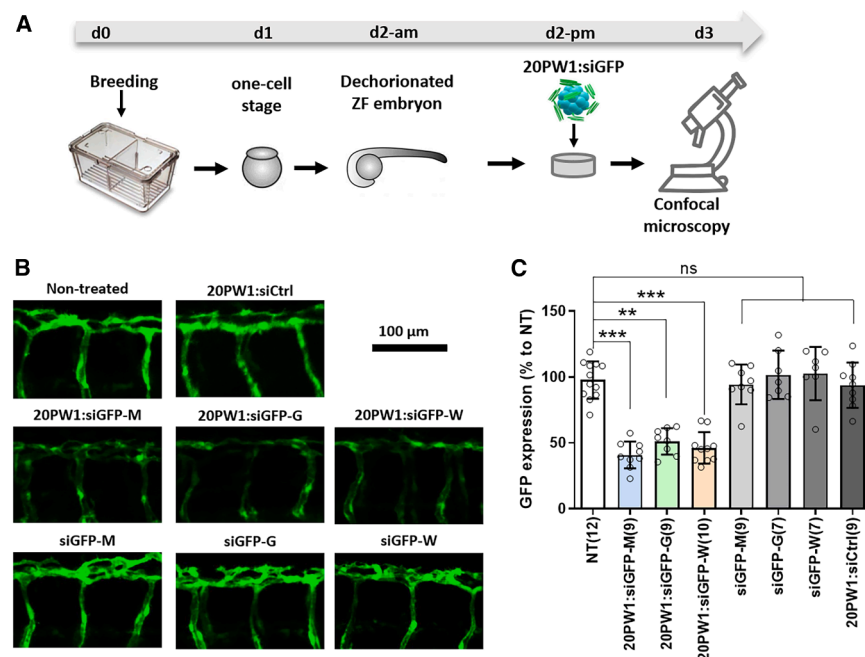


**Figure 6. Visualization of the GFP silencing in zebrafish embryos by 20% PEG-WRAP1:siRNA nanoparticle bathing**

(A) Schematic representation of the zebrafish embryo incubation protocol. At day zero (d0), zebrafish breeding was performed to collect one-cell stage embryos at d1. In the morning of d2 (~24 hpf), the zebrafish embryos were dechorionated and left for 6 h in E3 medium before adding in the afternoon the fluorescence-labeled 20% PEG-WRAP1:siRNA (20PW1:siGFP) nanoparticles. After ~20 h, the embryos were washed, fixed (PFA), and imaged by confocal microscopy. (B) Representative images of the z stack confocal microscopy acquisition of non-treated zebrafish embryo compared with those incubated with 20% PEG-WRAP1:siGFP and 20% PEG-WRAP1:siCtrl nanoparticles or with the siRNA alone. The final siRNA concentration was 140 nM for all conditions. Green = GFP-expressing endothelial cells. White bar = 100  $\mu$ m. (C) Quantification of the GFP fluorescence signal intensity of the conditions shown in (B). Brackets indicate the number of zebrafish embryos analyzed. Statistical evaluation: ns > 0.5, \*\* $p$  < 0.01, and \*\*\* $p$  < 0.001 vs. non-treated embryos (NT).

we determined the optimal siRNA dose and incubation time (24 h vs. 48 h) (Figure S4). Finally, significant GFP silencing was quantified for all three WRAP:siGFP nanoparticles by western blot (more than 60%) (Figure 5) and by confocal microscopy (about 50%) (Figure 6) compared with the control conditions (WRAP:siCtrl or the siGFP alone). We selected specifically the western blot assay to evaluate knockdown at the protein level given the fact that only a fraction of RNA-induced silencing complexes (RISCs) are capable of carrying out small RNA-directed RNA cleavage, while the remainder suppresses expression by interfering with protein synthesis. Consequently, evaluating knockdown exclusively through the measurement of RNA levels (e.g., by quantitative PCR or northern blotting) can potentially lead to an overestimation of knockdown for long-lived proteins or an underestimation of knockdown caused by contributions from non-catalytic RISCs.<sup>40</sup>

Zebrafish embryos between 0 hpf and 72 hpf (=3 days) have a closed mouth (feeding through the yolk). Oral absorption and excretion are fully functional only between 72 hpf and 126 hpf, when zebrafish morphogenesis is complete.<sup>41</sup> Since the PEGylated WRAP nanoparticles in our case were incubated by immersion with the zebrafish embryo between 48 hpf and 72 hpf, it is most likely that internalization is mainly by dermal translocation and not by oral adsorption.

The specificity of the GFP silencing by the siRNAs was controlled by a blast search of zebrafish nucleotides, which revealed some potential off-targets for siGFP-G and siGFP-W (see supplemental results). Slightly higher GFP knockdown observed in zebrafish embryos (~60%) compared with GFP-overexpressing HEK293 cells (~50%) could be explained by different promoters (CMV for the HEK293 cells vs. flil1 for the zebrafish embryos) resulting in a higher GFP expression

level in the HEK293 cells. Finally, the knockdown efficiencies for the three 20% PEG-WRAP1:siGFP nanoparticles measured by western blot analysis seemed to be more important than those quantified by confocal microscopy. However, GFP quantification by the two methods could not be directly compared because the GFP detection (fluorescence vs. antibody) is completely different, and more probably, the antibody detection may be more sensitive.

One potential strategy to improve the efficacy of RNAi-based silencing involves using chemically modified siRNAs. This approach involves the development of three modifications designed to diminish the siRNA degradation by ribonucleases. These modifications encompass alterations to the ribose (e.g., locked nucleic acid [LNA]), the phosphate (e.g., phosphorothioate [PS]), and base modifications (e.g., pseudouridine).<sup>42</sup> It is imperative to consider these modifications when conducting further *in vivo* studies.

There are many advantages in zebrafish handling, such as conserved vertebrate biology, ease of husbandry, high fecundity, small size, rapid development, and transparent juveniles. The zebrafish genome has been sequenced, and it has been shown that 70% of human genes have a zebrafish homolog, and more remarkably, 82% of human genes associated with the disease are mapped to a homologous gene in zebrafish.<sup>43</sup> For these reasons, zebrafish have long been studied for embryology, cell biology, genetics, and toxicology. Most toxicology studies on zebrafish have been focused on environmental pollutants, but there are also an increasing number of studies in the field of pharmaceutical toxicology.<sup>44</sup>

For all these studies, the incubation of zebrafish embryos by immersion in media containing various compounds or nanoparticles has

already been reported, with inconclusive results in most cases. For instance, Guarin et al. evaluated the spatiotemporal distribution of seven fluorescent alkyne compounds following immersion or microinjection (pericardial cavity, intraperitoneally, and yolk sac) of 72 hpf zebrafish embryos. The results of this study indicated that after 48 h, less signal was observed with immersion compared with microinjection.<sup>45</sup> Another example is given with different functionalized mesoporous silica nanoparticles (MSNs), which were incubated with zebrafish embryos by immersion. Confocal microscopy revealed that only polyethyleneimine-MSNs penetrated the embryos, whereas amino-, succinic acid-, or polyethyleneglycol-MSNs remained aggregated on the skin surface.<sup>46</sup>

In a study by van Pomerén et al.,<sup>47</sup> the authors evaluated the uptake of polystyrene particles of different sizes (25, 50, 250, and 700 nm) by immersion of zebrafish embryo. Irrespective of the size, internalization of the particles occurs only through oral uptake (between 72 and 120 hpf), which leads to dispersion in the body and ultimately to accumulation in certain organs such as the eyes or the digestive tract. Similar results were observed in adult zebrafish having a bath administration of surfactant-free poly(lactic acid) nanoparticles (PLA-NPs, 200 nm). Penetration and translocation through epithelial barriers were observed only from all exposed mucosae (gills, thymus, intestines, and the olfactory mucosa) and not from the fish skin.<sup>48</sup>

We recognize that the transfection of zebrafish embryos is not trivial and depends on the appropriate delivery systems, especially for skin transfection in the first-hour postfertilization. Here, we present the efficient skin transfection of siRNA via PEGylated WRAP1 using a simple immersion protocol showing a remarkable silencing effect exemplified by the GFP knockdown. Since the WRAP-based delivery system can encapsulate any siRNA, this technique could be useful in studying molecular interactions in early zebrafish embryo development and associated pathologies. It also opens up possibilities for novel RNAi-based pharmacological developments.

## MATERIALS AND METHODS

### Materials

WRAP1 (W1) and WRAP5 (W5) peptides were synthesized on the SynBio3 platform (Institut des Biomolécules Max Mousseron Montpellier) and crude products were purified in-house following a qualitative analysis by high-performance liquid chromatography/mass spectrometry as reported elsewhere.<sup>13</sup> PEG-WRAP1 (PW1) and PEG-WRAP5 (PW5) peptides were synthesized by coupling a PEG moiety to the N-terminal end of the WRAP peptide on resin, as described in more detail in the [supplemental information](#). Peptide stock solutions were prepared in pure water (Sigma-Aldrich) and stored at 4°C. The different siRNA sequences (unlabeled and Cy3-labeled) were purchased from Eurogentec (see [Table S1](#)), resuspended in RNase-free water, and stored at -20°C. The siRNA stock solutions were prepared in RNase-free water. Stably transfected GFP HEK293 cell lines were used. As antibodies, we used anti-rabbit (#600-401-215, Rockland), anti-Vinculin rabbit mAb E1E9V (#13901, Cell Signaling), anti- $\alpha$ -actinin (#3134, Cell Signaling), and

anti-rabbit immunoglobulin (Ig)G horseradish peroxidase (HRP) (#7074S, Cell Signaling).

### Nanoparticle formation

Nanoparticle formation was performed in pure water supplemented by 5% glucose (G7021, Sigma-Aldrich) by adding first the peptide and then the corresponding amount of siRNA at a molar ratio (MR) of 20:1 (peptide:siRNA) at room temperature.

### DLS and Zeta potential

Peptide:siRNA nanoparticles (peptide = 10  $\mu$ M, siRNA = 500 nM, MR = 20) were evaluated with a Zetasizer NanoZS (Malvern) in terms of mean size (Z-average) of the particle distribution and of homogeneity (Pdl). Zeta potential was determined in 5% glucose complemented with 1 mM or 5 mM NaCl (S5886, Sigma-Aldrich). All results were obtained from three independent measurements (three runs for each measurement at 25°C) using the Zetasizer software 7.11.

### Agarose gel shift retardation assay

WRAP:siRNA complexes (siRNA = 3.5  $\mu$ M in 20  $\mu$ L of an aqueous solution containing 5% glucose) were formed at a peptide:siRNA ratio of 20:1 and pre-incubated for 30 min at room temperature. Then, 5  $\mu$ L of heparin (H3149, Sigma-Aldrich) solutions were added to obtain a final concentration of 100  $\mu$ M, 50  $\mu$ M, 25  $\mu$ M, 12.5  $\mu$ M, and 6.25  $\mu$ M and again incubated for 30 min at room temperature. Finally, 20  $\mu$ L of each solution was loaded on an agarose gel (1% w/v, A9539, Sigma-Aldrich) and electrophoresis was performed at 50 V for 25 min. To visualize the siRNA, the agarose gel was stained with GelRed (BY1740, Interchim) for UV detection, and images were acquired using a FAS-Digi PRO Gel Imaging System imager (Nippon Genetics) equipped with a DMC-GF7 camera (Panasonic). The signal intensities were quantified using ImageJ software (gel analysis tool) (version 1.54m). Each band intensity corresponding to a distinguished condition was then normalized to the band intensity of the siRNA alone (=100%): Relative fluorescence (%) = fluorescence intensity (condition x)/fluorescence intensity (siRNA alone)  $\times$  100.

### Cell culture and transfection conditions

HEK293 (human embryonic kidney) cells stably transfected with an integrative GFP encoding plasmid were grown in a complete medium: DMEM with L-glutamine/pyruvate (COR10-013-CV, Ozyme), 1% penicillin/streptomycin (P4333, Sigma-Aldrich), and 10% heat-inactivated fetal bovine serum (FBS, P40-37500A, Dutscher). For western blot assay, 100,000 HEK293-GFP cells were seeded 24 h before the experiment into 24-well plates. The cells were incubated with 175  $\mu$ L of fresh pre-warmed serum-free DMEM +75  $\mu$ L of the nanoparticle solutions for standard incubation. After 1.5 h of incubation, 250  $\mu$ L DMEM supplemented with 20% FBS (final FBS concentration = 10%) was added to each well without withdrawing the transfection reagents. Cells were then incubated for another 24 h and finally lysed for western blotting (see below).

### Zebrafish experiments

Zebrafishes (*Danio rerio*) were raised and used according to standard laboratory protocols. Zebrafish use was performed in agreement with European Union guidelines for the handling of laboratory animals. All experiments were approved by the Comité d’Ethique pour l’Expérimentation Animale and the Direction Sanitaire et Vétérinaire de l’Hérault (Aquatic model facility, ZEFIX from CRBM C-34-172-39). *Tg[fli1:EGFP]<sup>v1</sup>* transgenic line was used with enhanced GFP-labeling of all endothelial cells.<sup>29</sup>

Zebrafish embryos were kept for 24 h in a dish (100 mm) in E3 medium (5 mM NaCl, 0.17 mM KCl, 0.33 mM CaCl<sub>2</sub>, 0.33 mM MgSO<sub>4</sub>, 0.01 mg/L methylene blue) in an incubator at 28°C. Thereafter, the zebrafish embryo chorions were removed with sharp forceps and the embryos were kept in an E3 medium containing 75 µM N-Phenylthiourea (PTU, P7629, Sigma-Aldrich) to avoid pigment formation. Six hours after chorion removal, zebrafish embryos were washed twice with E3+PTU medium and then incubated with the nanoparticles for 24 h at 28°C. The nanoparticles were formulated at a peptide:siRNA molar ratio of 20:1 (see the preceding section “nanoparticle formation”) with an siRNA concentration of 3 mM and then directly diluted in the E3+PTU medium at the desired siRNA concentration. For western blot analysis or confocal microscopy imaging, zebrafish embryos were previously washed twice with E3+PTU medium before proceeding (see the following sections). Three independent experiments were performed with 3–5 zebrafish embryos per condition.

### Relative viability measurement

The Cytotoxicity Detection Kit<sup>Plus</sup> (LDH, #04744934001, Sigma-Aldrich) was used to evaluate the cytotoxicity induced by the PBNs. After the PBN incubation (36 h), at least one well was used as LDH negative control (0% viability) by adding Triton X-100 (T9797, Sigma-Aldrich) to a final concentration of 0.1% (~15 min incubation at 37°C). Non-treated cells were considered as 100% viability (= positive control). Afterward, 50 µL supernatant of each well was transferred in a new clear 96-well plate (Greiner) and completed with 50 µL/well of the “dye solution/catalyst” mixture as recommended by the manufacturer. The plate was then incubated in the dark for 30 min at room temperature. The reaction was stopped by adding 25 µL/well of HCl (1 N) before measuring the absorption at 490 nm using the Infinite M200 pro plate reader (Tecan). Relative viability (%) was calculated with the following formula:  $[100 - ((\text{value treated cells} - \text{value non-treated cells}) / (\text{value Triton} - \text{value non-treated cells}) \times 100)]$ .

### Western blot

#### HEK293-GFP cells

Transfected cells were lysed in 130 µL/24-well RIPA buffer (50 mM Tris pH 8.0, 150 mM NaCl, 1% Triton X-100, 0.1% SDS [sodium dodecyl sulfate, L4509, Sigma-Aldrich], including SigmaFAST protease inhibitor cocktail [diluted 1/10, S8820, Sigma-Aldrich]) on ice for 5 min. Thereafter, cells were scraped and transferred in a 1.5-mL tube and kept a further 5 min on ice.

### Zebrafish embryos

At 48 hpf (= 24 h post PBN incubation), one embryo was placed in one 1.5-mL tube. Embryos were de-yolked using an ice-cold Ringer solution (11.6 mM NaCl, 0.29 mM KCl, 0.18 mM CaCl<sub>2</sub>,<sup>2</sup> 0.5 mM HEPES, pH 7.2) by triturating with a P200 pipette. The de-yolked embryo was rinsed twice with the same Ringer solution before adding 70 µL RIPA buffer (see above). The embryos were incubated on a rotating wheel at 4°C for complete lysis, followed by a sonication step of 20 min.

Afterward, for both sample types (from cells or zebrafish embryos), lysates were centrifuged (10 min, 13,500 × g, 4°C), supernatants were collected in novel tubes and protein concentrations were determined using the Pierce BCA Protein Assay (#23225, Thermo Fisher). Proteins (15 µg and 8 µg from cell and zebrafish embryo lysates, respectively) were separated by 4%–20% Mini-PROTEAN TGXTM Precast Gels (#4561094 or #4561095, Bio-Rad) and transferred onto Trans-Blot Turbo PVDF Transfer Membranes (#1704157, Bio-Rad). Primary and secondary antibodies were incubated in 5% BSA TBS-T buffer overnight at 4°C or for 1 h at room temperature, respectively. Western blots were revealed with the Pierce ECL plus western blotting substrate (Thermo Fisher) on an Amersham imager 600 (GE Healthcare Life Science). The signal intensities of the blots were quantified using ImageJ software (version 1.54m). Each band intensity corresponding to a distinguished condition is then normalized to the band intensity of non-treated cells (NT) (= 100%): Relative Signal Intensity (%) = intensity (condition x)/intensity (NT) × 100.

### Confocal microscopy

Zebrafish embryos were fixed in 4% PFA in phosphate-buffered saline (PBS) for 30 min at room temperature. Afterward, embryos were washed five times with PBS buffer and kept in PBS buffer at 4°C until imaging. Image acquisition was performed by confocal microscopy on an inverted Zeiss LSM800 microscope using a lens Apo 63x/1.2 W DICIII. All confocal acquisitions were performed using a diode laser 488 nm with the specific GFP filter (486 nm–561 nm) and a diode laser 561 nm with the specific Alexa 594 filter (592 nm–614 nm). Fifteen images per sample were acquired using z stack mode with a z stack interval of 3 µm. Acquired images were analyzed using the ImageJ software (version 1.54m). Z projection for each sample was performed by summing fluorescence intensities to one image. The threshold of each sample was adjusted to quantify the mean fluorescence of the image.

### Statistical evaluation

Statistical analysis was performed only for independent experiments. Data (mean ± SD) were analyzed with an ordinary one-way ANOVA and the Dunnett’s post-test. Data were analyzed with GraphPad Prism version 8.0.2.

### ACKNOWLEDGMENTS

This research was funded by the “Fondation ARC pour la Recherche sur le Cancer” (PJA20171206171 to P.B.), the “Agence Nationale de la Recherche” (ANR-21-CE18-0022-01 to P.B.), AFM-Téléthon (n 23800 to S.F.), and by institutional funds from

Inserm, CNRS, and University of Montpellier. The authors are grateful to Pascal Verdié from the SynBio3 platform for providing peptide synthesis facilities, and to Pierre Sanchez for performing LCMS analysis, both from the Institut des Biomolécules Max Mousseron (IBMM), Montpellier (France). The authors thank Marc Plays and Bénédicte Delaval from the Aquatic model platform ZEFIX situated at the Cell Biology Research of Montpellier (CRBM) for technical support.

## AUTHOR CONTRIBUTIONS

Conceptualization, S.Deshayes and P.B.; methodology and formal analysis, C.T.A., K.K., S. Descamps, E.V., S. Deshayes, I.P., T.H., and P.B.; writing – original draft preparation, P.B.; writing – review and editing, E.V., K.K., S. Deshayes, S.F., and P.d.S.B.; funding acquisition, P.B., S.F., and P.d.S.B. All authors have read and agreed to the published version of the manuscript.

## DECLARATION OF INTERESTS

Patent entitled “Non-naturally occurring peptides for use as cell-penetrating peptides” WO2020/016242.

## SUPPLEMENTAL INFORMATION

Supplemental information can be found online at <https://doi.org/10.1016/j.omtm.2025.101458>.

## REFERENCES

- Talap, J., Zhao, J., Shen, M., Song, Z., Zhou, H., Kang, Y., Sun, L., Yu, L., Zeng, S., and Cai, S. (2021). Recent advances in therapeutic nucleic acids and their analytical methods. *J. Pharm. Biomed. Anal.* 206, 114368. <https://doi.org/10.1016/j.jpba.2021.114368>.
- Tolia, N.H., and Joshua-Tor, L. (2007). Slicer and the argonautes. *Nat. Chem. Biol.* 3, 36–43. <https://doi.org/10.1038/nchembio484>.
- Whitehead, K.A., Langer, R., and Anderson, D.G. (2009). Knocking down barriers: advances in siRNA delivery. *Nat. Rev. Drug Discov.* 8, 129–138. <https://doi.org/10.1038/nrd2742>.
- Tang, Q., and Khvorova, A. (2024). RNAi-based drug design: considerations and future directions. *Nat. Rev. Drug Discov.* 23, 341–364. <https://doi.org/10.1038/s41573-024-00912-9>.
- Hoy, S.M. (2018). Patisiran: First Global Approval. *Drugs* 78, 1625–1631. <https://doi.org/10.1007/s40265-018-0983-6>.
- Paunovska, K., Loughrey, D., and Dahlman, J.E. (2022). Drug delivery systems for RNA therapeutics. *Nat. Rev. Genet.* 23, 265–280. <https://doi.org/10.1038/s41576-021-00439-4>.
- Roberts, T.C., Langer, R., and Wood, M.J.A. (2020). Advances in oligonucleotide drug delivery. *Nat. Rev. Drug Discov.* 19, 673–694. <https://doi.org/10.1038/s41573-020-0075-7>.
- Boisguérin, P., Deshayes, S., Gait, M.J., O'Donovan, L., Godfrey, C., Betts, C.A., Wood, M.J.A., and Lebleu, B. (2015). Delivery of therapeutic oligonucleotides with cell penetrating peptides. *Adv. Drug Deliv. Rev.* 87, 52–67. <https://doi.org/10.1016/j.addr.2015.02.008>.
- Lehto, T., Ezzat, K., Wood, M.J.A., and El Andaloussi, S. (2016). Peptides for nucleic acid delivery. *Adv. Drug Deliv. Rev.* 106, 172–182. <https://doi.org/10.1016/j.addr.2016.06.008>.
- Kurrikoff, K., and Langel, Ü. (2019). Recent CPP-based applications in medicine. *Expert Opin. Drug Deliv.* 16, 1183–1191. <https://doi.org/10.1080/17425247.2019.1665021>.
- Boisguérin, P., Konate, K., Josse, E., Vivès, E., and Deshayes, S. (2021). Peptide-Based Nanoparticles for Therapeutic Nucleic Acid Delivery. *Biomedicines* 9, 583. <https://doi.org/10.3390/biomedicines9050583>.
- Pasut, G., and Veronese, F.M. (2012). State of the art in PEGylation: the great versatility achieved after forty years of research. *J. Control. Release* 161, 461–472. <https://doi.org/10.1016/j.jconrel.2011.10.037>.
- Konate, K., Dussot, M., Aldrian, G., Vaissière, A., Viguier, V., Neira, I.F., Couillaud, F., Vivès, E., Boisguérin, P., and Deshayes, S. (2019). Peptide-Based Nanoparticles to Rapidly and Efficiently “Wrap ‘n Roll” siRNA into Cells. *Bioconjug. Chem.* 30, 592–603. <https://doi.org/10.1021/acs.bioconjchem.8b00776>.
- Deshayes, S., Konate, K., Dussot, M., Chavey, B., Vaissière, A., Van, T.N.N., Aldrian, G., Padari, K., Pooga, M., Vivès, E., and Boisguérin, P. (2020). Deciphering the internalization mechanism of WRAP:siRNA nanoparticles. *Biochim. Biophys. Acta. Biomembr.* 1862, 183252. <https://doi.org/10.1016/j.bbmem.2020.183252>.
- Konate, K., Josse, E., Tasic, M., Redjatti, K., Aldrian, G., Deshayes, S., Boisguérin, P., and Vivès, E. (2021). WRAP-based nanoparticles for siRNA delivery: a SAR study and a comparison with lipid-based transfection reagents. *J. Nanobiotechnology* 19, 236. <https://doi.org/10.1186/s12951-021-00972-8>.
- Ferreiro, I., Genevois, C., Konate, K., Vivès, E., Boisguérin, P., Deshayes, S., and Couillaud, F. (2021). In Vivo Follow-Up of Gene Inhibition in Solid Tumors Using Peptide-Based Nanoparticles for siRNA Delivery. *Pharmaceutics* 13, 749. <https://doi.org/10.3390/pharmaceutics13050749>.
- Molla, M.R., Chakraborty, S., Munoz–Sagredo, L., Drechsler, M., Orian–Rousseau, V., and Levkin, P.A. (2020). Combinatorial Synthesis of a Lipidoid Library by Thiolactone Chemistry: In Vitro Screening and In Vivo Validation for siRNA Delivery. *Bioconjug. Chem.* 31, 852–860. <https://doi.org/10.1021/acs.bioconjchem.0c00013>.
- Gruber, J., Manninga, H., Tuschl, T., Osborn, M., and Weber, K. (2005). Specific RNAi Mediated Gene Knockdown in Zebrafish Cell Lines. *RNA Biol.* 2, 101–105. <https://doi.org/10.4161/rna.2.3.2060>.
- Wen, Y., Bai, H., Zhu, J., Song, X., Tang, G., and Li, J. (2020). A supramolecular platform for controlling and optimizing molecular architectures of siRNA targeted delivery vehicles. *Sci. Adv.* 6, eabc2148. <https://doi.org/10.1126/sciadv.abc2148>.
- Allen, C., Dos Santos, N., Gallagher, R., Chiu, G.N.C., Shu, Y., Li, W.M., Johnstone, S.A., Janoff, A.S., Mayer, L.D., Webb, M.S., and Bally, M.B. (2002). Controlling the physical behavior and biological performance of liposome formulations through use of surface grafted poly(ethylene glycol). *Biosci. Rep.* 22, 225–250. <https://doi.org/10.1023/a:1020186505848>.
- Aldrian, G., Vaissière, A., Konate, K., Seisel, Q., Vivès, E., Fernandez, F., Viguier, V., Genevois, C., Couillaud, F., Déménè, H., et al. (2017). PEGylation rate influences peptide-based nanoparticles mediated siRNA delivery in vitro and in vivo. *J. Control. Release* 256, 79–91. <https://doi.org/10.1016/j.jconrel.2017.04.012>.
- Faria, R., Vivès, E., Boisguérin, P., Descamps, S., Sousa, Â., and Costa, D. (2024). Upgrading Mitochondria-Targeting Peptide-Based Nanocomplexes for Zebrafish In Vivo Compatibility Assays. *Pharmaceutics* 16, 961. <https://doi.org/10.3390/pharmaceutics16070961>.
- Di Gregorio, G., Coléo, V., Karidia, K., Clémentine, T.-A., Hammoum, T.F., Gautron, H., Bessin, Y., Deshayes, S., Vivès, E., Meli, A.C., et al. (2025). Enhancing WRAP-based nanoparticles for siRNA delivery in pH-sensitive environments. *ChemMedChem*, e202400885. <https://doi.org/10.1002/cmdc.202400885>.
- Porosk, L., Härk, H.H., Arukuusk, P., Haljasorg, U., Peterson, P., and Kurrikoff, K. (2023). The Development of Cell-Penetrating Peptides for Efficient and Selective In Vivo Expression of mRNA in Spleen Tissue. *Pharmaceutics* 15, 952. <https://doi.org/10.3390/pharmaceutics15030952>.
- Karlsson, J., von Hofsten, J., and Olsson, P.E. (2001). Generating transparent zebrafish: a refined method to improve detection of gene expression during embryonic development. *Mar. Biotechnol.* 3, 522–527. <https://doi.org/10.1007/s1012601-0053-4>.
- Schnabel, D., Castillo-Robles, J., and Lomeli, H. (2019). Protein Purification and Western Blot Detection from Single Zebrafish Embryo. *Zebrafish* 16, 505–507. <https://doi.org/10.1089/zeb.2019.1761>.
- Purushothaman, K., Das, P.P., Presslauer, C., Lim, T.K., Johansen, S.D., Lin, Q., and Babiak, I. (2019). Proteomics Analysis of Early Developmental Stages of Zebrafish Embryos. *Int. J. Mol. Sci.* 20, 6359. <https://doi.org/10.3390/ijms20246359>.
- Corish, P., and Tyler-Smith, C. (1999). Attenuation of green fluorescent protein half-life in mammalian cells. *Protein Eng.* 12, 1035–1040. <https://doi.org/10.1093/protein/12.12.1035>.
- Lawson, N.D., and Weinstein, B.M. (2002). In Vivo Imaging of Embryonic Vascular Development Using Transgenic Zebrafish. *Dev. Biol.* 248, 307–318. <https://doi.org/10.1006/dbio.2002.0711>.



30. Veiman, K.-L., Künnapuu, K., Lehto, T., Kiisholts, K., Pärn, K., Langel, Ü., and Kurrikoff, K. (2015). PEG shielded MMP sensitive CPPs for efficient and tumor specific gene delivery in vivo. *J. Control. Release* 209, 238–247. <https://doi.org/10.1016/j.jconrel.2015.04.038>.
31. Kurrikoff, K., Veiman, K.-L., Künnapuu, K., Peets, E.M., Lehto, T., Pärnaste, L., Arukuusk, P., and Langel, Ü. (2017). Effective in vivo gene delivery with reduced toxicity, achieved by charge and fatty acid -modified cell penetrating peptide. *Sci. Rep.* 7, 17056. <https://doi.org/10.1038/s41598-017-17316-y>.
32. Intermolecular and Surface Forces - 3rd Edition <https://www.elsevier.com/books/intermolecular-and-surface-forces/israelachvili/978-0-12-391927-4>.
33. Takács, D., Tomšić, M., and Szilagy, I. (2022). Effect of Water and Salt on the Colloidal Stability of Latex Particles in Ionic Liquid Solutions. *Colloids Interfaces* 6, 2. <https://doi.org/10.3390/colloids6010002>.
34. Bizmark, N., and Ioannidis, M.A. (2015). Effects of Ionic Strength on the Colloidal Stability and Interfacial Assembly of Hydrophobic Ethyl Cellulose Nanoparticles. *Langmuir* 31, 9282–9289. <https://doi.org/10.1021/acs.langmuir.5b01857>.
35. Pamies, R., Cifre, J.G.H., Espín, V.F., Collado-González, M., Baños, F.G.D., and de la Torre, J.G. (2014). Aggregation behaviour of gold nanoparticles in saline aqueous media. *J. Nanoparticle Res.* 16, 2376. <https://doi.org/10.1007/s11051-014-2376-4>.
36. Lee, H. (2020). Molecular Simulations of PEGylated Biomolecules, Liposomes, and Nanoparticles for Drug Delivery Applications. *Pharmaceutics* 12, E533. <https://doi.org/10.3390/pharmaceutics12060533>.
37. Li, D., Wang, F., Di, H., Liu, X., Zhang, P., Zhou, W., and Liu, D. (2019). Cross-Linked Poly(ethylene glycol) Shells for Nanoparticles: Enhanced Stealth Effect and Colloidal Stability. *Langmuir* 35, 8799–8805. <https://doi.org/10.1021/acs.langmuir.9b01325>.
38. Hristov, D.R., Lopez, H., Ortin, Y., O'Sullivan, K., Dawson, K.A., and Brougham, D. F. (2021). Impact of dynamic sub-populations within grafted chains on the protein binding and colloidal stability of PEGylated nanoparticles. *Nanoscale* 13, 5344–5355. <https://doi.org/10.1039/d0nr08294e>.
39. Shi, L., Zhang, J., Zhao, M., Tang, S., Cheng, X., Zhang, W., Li, W., Liu, X., Peng, H., and Wang, Q. (2021). Effects of polyethylene glycol on the surface of nanoparticles for targeted drug delivery. *Nanoscale* 13, 10748–10764. <https://doi.org/10.1039/d1nr02065j>.
40. Chang, K., Marran, K., Valentine, A., and Hannon, G.J. (2012). RNAi in Cultured Mammalian Cells Using Synthetic siRNAs. *Cold Spring Harb. Protoc.* 2012, 957–961. <https://doi.org/10.1101/pdb.prot071076>.
41. Ng, A.N.Y., de Jong-Curtain, T.A., Mawdsley, D.J., White, S.J., Shin, J., Appel, B., Dong, P.D.S., Stainier, D.Y.R., and Heath, J.K. (2005). Formation of the digestive system in zebrafish: III. Intestinal epithelium morphogenesis. *Dev. Biol.* 286, 114–135. <https://doi.org/10.1016/j.ydbio.2005.07.013>.
42. Chernikov, I.V., Ponomareva, U.A., and Chernolovskaya, E.L. (2023). Structural Modifications of siRNA Improve Its Performance In Vivo. *Int. J. Mol. Sci.* 24, 956. <https://doi.org/10.3390/ijms24020956>.
43. Howe, K., Clark, M.D., Torroja, C.F., Torrance, J., Berthelot, C., Muffato, M., Collins, J.E., Humphray, S., McLaren, K., Matthews, L., et al. (2013). The zebrafish reference genome sequence and its relationship to the human genome. *Nature* 496, 498–503. <https://doi.org/10.1038/nature12111>.
44. Cassar, S., Adatto, I., Freeman, J.L., Gamse, J.T., Iturria, I., Lawrence, C., Muriana, A., Peterson, R.T., Van Cruchten, S., and Zon, L.I. (2020). Use of Zebrafish in Drug Discovery Toxicology. *Chem. Res. Toxicol.* 33, 95–118. <https://doi.org/10.1021/acs.chemrestox.9b00335>.
45. Guarin, M., Faelens, R., Giusti, A., De Croze, N., Léonard, M., Cabooter, D., Annaert, P., de Witte, P., and Ny, A. (2021). Spatiotemporal imaging and pharmacokinetics of fluorescent compounds in zebrafish cleuthero-embryos after different routes of administration. *Sci. Rep.* 11, 12229. <https://doi.org/10.1038/s41598-021-91612-6>.
46. Paatero, I., Casals, E., Niemi, R., Özliseli, E., Rosenholm, J.M., and Sahlgren, C. (2017). Analyses in zebrafish embryos reveal that nanotoxicity profiles are dependent on surface-functionalization controlled penetrance of biological membranes. *Sci. Rep.* 7, 8423. <https://doi.org/10.1038/s41598-017-09312-z>.
47. van Pomerén, M., Brun, N.R., Peijnenburg, W.J.G.M., and Vijver, M.G. (2017). Exploring uptake and biodistribution of polystyrene (nano)particles in zebrafish embryos at different developmental stages. *Aquat. Toxicol.* 190, 40–45. <https://doi.org/10.1016/j.aquatox.2017.06.017>.
48. Rességuier, J., Delaune, E., Coolen, A.-L., Levraud, J.-P., Boudinot, P., Le Guellec, D., and Verrier, B. (2017). Specific and Efficient Uptake of Surfactant-Free Poly(Lactic Acid) Nanovaccine Vehicles by Mucosal Dendritic Cells in Adult Zebrafish after Bath Immersion. *Front. Immunol.* 8, 190. <https://doi.org/10.3389/fimmu.2017.00190>.